Phase behavior of isolated skin lipids

J. A. Bouwstra,[1],* G. S. Gooris,* K. Cheng,* A. Weerheim,[§] W. Bras,[†] and M. Ponec[§]

Leiden/Amsterdam Center for Drug Research,* Gorlaeus Laboratories, Leiden University, P.O. Box 9502, 2300 RA Leiden, The Netherlands; NWO/SERC Daresbury Laboratory,[†] Warrington, WA4 4AD, United Kingdom; and Department of Dermatology,[§] University Hospital, Leiden, The Netherlands

Abstract Ceramides were isolated from the pig stratum corneum (SC) and mixed in varying molar ratios with either cholesterol or with cholesterol and free fatty acids. The phase behavior of the mixtures was studied by small-(SAXD) and wide-angle (WAXD) X-ray diffraction. Ceramides alone did not exhibit a long range ordering. Upon addition of cholesterol to ceramides, lamellar phases were formed and a hexagonal lateral packing was detected similar to that seen in intact SC. At a cholesterol/ceramide molar ratio of 0.1, only one reflection at 5.9 nm was observed. At a cholesterol/ceramide molar ratio of 0.2, three reflections corresponding to 12.3, 5.56, and 4.26 nm appeared. The reflections were based on two phases. Increasing the cholesterol/ceramide ratio to 0.4, the peak positions were slightly shifted. The diffraction pattern revealed the presence of two lamellar phases with periodicities of 12.2 and 5.2 nm, respectively. The positions of the peaks remained unchanged when the cholesterol/ceramide ratio was increased up to 1.0. At a cholesterol/ceramide molar ratio of 2.0, the intensity of various peaks based on the 12.2 nm phase decreased in intensity. The phase behavior of the cholesterol/ceramide mixtures in a ratio between 0.4 and 1.0 was very similar to that found in intact pig SC in which two lamellar phases with periodicities of 6.0 and 13.2 nm are present. Our data further indicate that the formation of the 5.2 nm lamellar phase requires a higher cholesterol content than the formation of the 12.2 nm lamellar phase. Furthermore, when the relative amount of cholesterol is very high, the 5.2 nm phase is the most pronounced one. Addition of free fatty acids increased the solubility of cholesterol, indicating the role free fatty acids may play for the skin barrier function. The phase behavior of cholesterol/ceramide/fatty acid mixtures was found to be dependent on the chain length of fatty acids used. Namely, addition of short-chain free fatty acids (C14–C18) did not change the periodicity of the 12.2 and 5.2 nm phases, but induced the formation of an additional 4.2 nm phase. In the presence of long-chain free fatty acids (C16–C26), the periodicity of the lamellar phases was slightly increased (to 13.0 and 5.3 nm, respectively) but no additional 4.2 nm phase was formed. These results indicate that the lipid phase behavior of the cholesterol/ceramide/free fatty acid mixtures closely mimics that of the intact stratum corneum only in the presence of long-chain free fatty acids.—**Bouwstra, J. A., G. S. Gooris, K. Cheng, A. Weerheim, W. Bras, and M. Ponec.** Phase behavior of isolated skin lipids. *J. Lipid Res.* 1996. **37:** 999–1011.

Supplementary key words stratum corneum • ceramides • phase behavior • X-ray diffraction • free fatty acids • cholesterol

The uppermost layer of the epidermis, the stratum corneum (SC), forms the main barrier for diffusion of substances through the skin. The SC is composed of protein-enriched corneocytes embedded in lipid-rich extracellular matrix. It is generally accepted that SC lipids play an important role for barrier integrity (1, 2). Up to now considerable effort has been undertaken to elucidate the organization of SC lipids. At the end of the fifties and early sixties the first extensive studies on SC lipid organization using X-ray diffraction were carried out (3, 4). The results were interpreted by proposing a model in which the SC lipids are surrounded by keratin filaments. They found that the lipids formed crystalline phases and that occasionally cholesterol crystallized in a separate phase. In the early seventies the SC ultrastructure was visualized by freeze fracture electron microscopy (5). It was reported that the lipids were not surrounding the keratin filaments by forming tube-like structures, but that lipids formed lamellae within the intercellular spaces. More than 10 years later the presence of stacks of intercellular bilayers was confirmed with RuO_4 post-fixation technique used in combination with transmission electron microscopy (6). With this technique a very exceptional organization pattern of the SC bilayers was observed. The membrane complex was found to consist of two broad and one narrow electron-lucent bands. The existence of the broad-narrow-broad pattern indicates that the repeating unit in the direction perpendicular to the basal plane of the lamellae consists

Abbreviations: CER, ceramides; CHOL, cholesterol; FFA, free fatty acids; SAXD, small-angle X-ray diffraction; WAXD, wide-angle X-ray diffraction; SC, stratum corneum; θ, scattering angle; λ, wave length; Q, scattering vector; d, periodicity.

[1]To whom correspondence should be addressed.

TABLE 1. Ceramide profile in pig stratum corneum

Ceramides	w/w %
1	7.8
2	55.4
3	17.6
4	3.6
5	9.9
6	5.6

of more than one bilayer which is in contrast to most biological membranes. Recent X-ray diffraction studies on the phase behavior of intact human, mouse, and pig SC revealed that *i)* two lamellar structures are present in the SC of human, pig, and mouse (7–10) with periodicities of approximately 6 and 13 nm, respectively, and *ii)* the lipid chain packing is liquid-like, hexagonal or orthorhombic (7, 9–11). The intercellular lipids that form lamellar bilayers consist mainly of ceramides (CER), cholesterol (CHOL), and free fatty acids (FFA) (12, 13). To gain insight in the phase behavior of SC lipids, X-ray diffraction patterns of lipids extracted from the SC were examined and compared with those obtained with intact SC. These studies revealed that phase behavior of the total SC lipid extracts and of the intact SC differed (7, 14). At present it is not clear whether the observed differences can be ascribed to the presence of variable amounts of other lipids, such as triglycerides, which may disturb the phase behavior of the main components of the intercellular lipid lamellae, CHOL, CER, FFA (12, 13), or to the absence of proteins, the absence of various ions, like calcium, and/or to the differences in pH.

As the quality of the SC barrier is most likely dependent on the SC lipid structure and composition (15–17), the present study was undertaken to examine the role various SC lipid classes play for proper organization of lipid bilayers. For this purpose ceramides were isolated from the pig SC and subsequently mixed with commercially available cholesterol in various molar ratios and the phase behavior of these mixtures was studied with small- and wide-angle X-ray diffraction. In addition, the effect of commercially available FFA on the phase behavior was studied in three component mixtures of FFA, CHOL, and CER.

MATERIALS AND METHODS

Isolation of stratum corneum from pig skin

Fresh pig skin was obtained from a slaughter house. First, the apical side of the skin was very briefly washed with hexane (0.03 ml/cm^2) in order to remove the surface lipids. Then the hairs were removed with a razor blade. The epidermis was separated from underlying epidermis by heating the tissue for 5 min at 60°C. The SC was isolated by trypsin digestion (0.1% in a phosphate-buffered saline solution).

Isolation of ceramides: extraction, separation and identification of lipids from stratum corneum

Epidermal lipids were extracted using the method of Bligh and Dyer (18), and the extracts were dissolved in chloroform–methanol 2:1 (v/v) and stored at -20°C under nitrogen until use. Subsequently, the extracted lipids were applied on a Silicagel 60 (Merck) column with a diameter of 2 cm and a length of 33 cm and various lipid classes were eluted sequentially using various solvent mixtures in the following sequence: 100 ml hexane–chloroform–diethylether 40:40:20, 200 ml hexane–chloroform–diethylether–2-propanol 40:40:20:1, 100 ml hexane–chloroform–diethylether–ethylacetate–2-propanol 40:37:20:2:1, 200 ml hexane–chloroform–diethylether – ethylacetate–2-propanol 20:35:39:5:1, 100 ml hexane – chloroform – diethylether – ethylacetate – methylethylketone – acetone – methanol 20:20:40:12:4:2:2, 100 ml hexane–chloroform–diethylether– ethylacetate – methylethylketone–acetone–methanol 20:20:30:6:12:8:4, 100 ml chloroform–acetone–methanol 75:20:5, 50 ml chloroform – diethylether – ethylacetate – methylethylketone–acetone–methanol 15:15:2:6:8:4, 50 ml chloroform–diethylether–acetone–methanol 20:12.5:10:7.5, 50 ml chloroform–diethylether–acetone–methanol 25:5:10:10, and 100 ml methanol. The eluted lipids were collected in either 10-ml fractions or 3-ml fractions, depending on whether or not ceramides were expected to be present in the fraction. The lipid composition of individual fractions was established by one-dimensional high performance thin layer chromatography, as de-

TABLE 2. Chain distribution of major non-hydroxy amide-linked fatty acids and the α-hydroxy amide-linked fatty acids of the ceramides

	Ceramides	
Alkyl Chain	Non-hydroxy Fatty Acids	α-Hydroxy Fatty Acids
14:0		2.6
16:0	3.1	45.7
18:0	30.	
18:1	2.8	
18:2	5.7	
20:0	12.0	11.5
22:0	11.5	6.3
24:0	25.8	27.7
25:0	2.8	
26:0	12.6	2.1
28:0	10.4	

Percentages are given in % w/w.

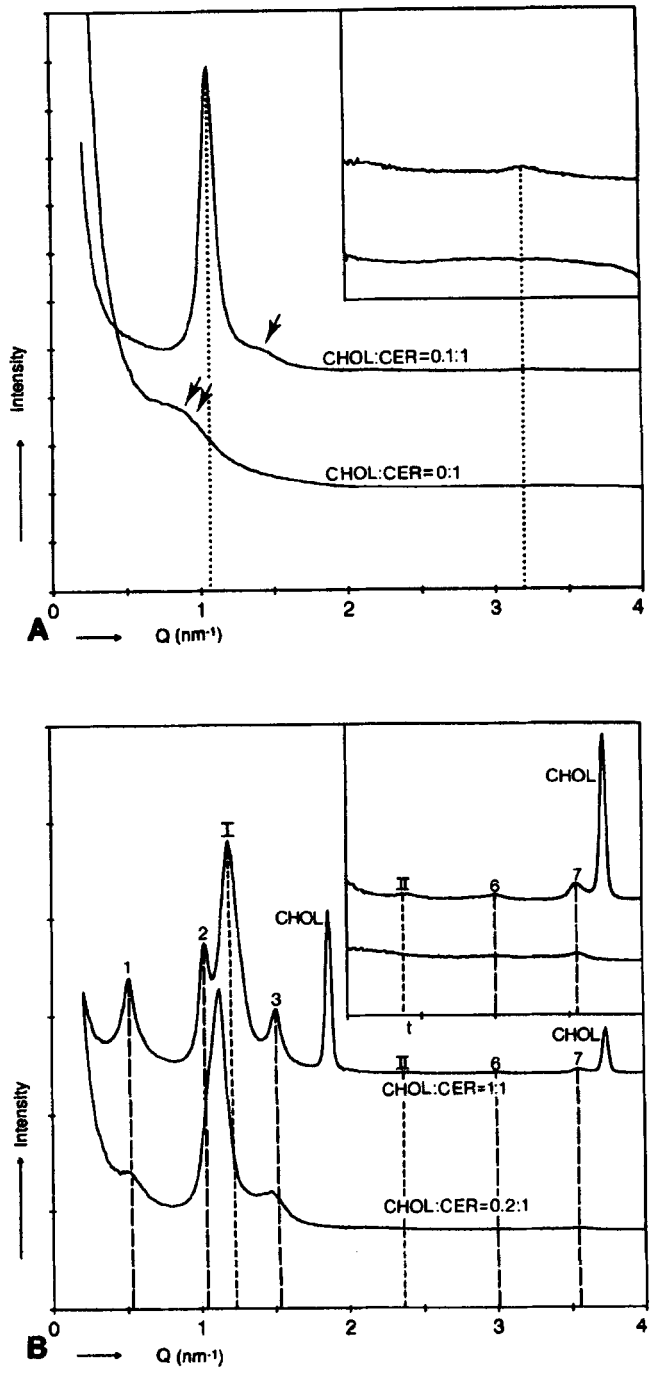

Fig. 1. Small angle X-ray diffraction curves of mixtures of cholesterol (CHOL) and ceramides (CER). A: CHOL:CER mixtures in a molar ratio of 0:1 and 0.1:1. Single arrow: the shoulder at approximately 4.3 nm spacing indicates the presence of the 12.2 nm phase. Double arrow: shoulder at the diffraction curve of ceramides. The dotted lines represent the first and third order of the 5.9 nm lamellar phase. B: CHOL:CER mixtures in molar ratios of 0.2:1 and 1:1. The numbers 1, 2, 3, 6, and 7 denote the various orders of the 12.2 nm phase; I and II denote the 1st and 2nd order of the 5.2 nm phase; CHOL denotes cholesterol. Inset: the scale for the intensity is different to show the weak intensity peaks.

scribed before (19). For quantification, authentic standards (Sigma) were run in parallel. The quantification was performed after charring using a photodensitometer with automatic peak integration (Desaga, Germany).

Preparation of lipid mixtures

Cholesterol (purchased from Sigma) and isolated pig SC ceramides were mixed in various molar ratios, using a mean ceramide molar weight of 700. For calculation of the mean ceramide molecular weight, the data on the ceramide composition and alkyl chain length distributions (20) were used. Approximately 2 mg of lipids was solubilized in 80 µl chloroform–methanol 2:1 at the desired composition and applied on mica at a very low rate (4.2 µl/min) under a stream of nitrogen using a sample applicator (CAMAG LINOMAT IV). The applied lipid mixtures were covered with 1–2 ml acetate buffer at pH 5.0 (10 mM) and kept under nitrogen. A pH 5 was chosen, as that is the pH of the skin surface (21). To reach homogeneous mixing of various lipid fractions, the lipids applied on mica were first heated to 80°C and kept at this temperature for 2–5 min. Subsequently, the samples were quenched using dry ice. Then the samples were placed in a small copper sample holder, after which at least 10 freeze-thawing cycles were carried out between -20°C and room temperature. Until use the samples were stored at -20°C. For preparation of the three component mixtures of ceramides/cholesterol and free fatty acids, the following free fatty acid mixtures (all purchased at Sigma) were used: *i)* a mixture of C18:0, C16:0, C14:0, C18:1, C18:2, and C16:1 fatty acids (all purchased at Sigma) was prepared by mixing fatty acids at molar ratios of 9.9:36.9:3.8:33.2:12.5:3.6 (22), respectively, referred to in this paper as the short-chain FFA; or *ii)* a mixture of C16:0, C18:0, C22:0, C22:3, C24:0, C26:0 fatty acids by mixing fatty acids at molar ratios of 1.3, 3.2, 41.7, 5.4, 36.8, and 6.9% (12), respectively, referred to in this paper as the long-chain FFA.

X-ray diffraction measurements

Small angle X-ray diffraction. All measurements were carried out at the Synchrotron Radiation Source at Daresbury Laboratory using station 8.2. This station has been built as a part of a NWO/SERC agreement. The samples were put in a specially designed sample holder with two mica windows. A detailed description of the equipment has been given elsewhere (8). Due to crystallinity, the sample exerts a granular appearance with thickness varying between 10 µm and 1 mm. In addition, no orientation of the lipid layers to the primary beam is achieved. This is caused by the crystallinity and the low water content in the lipid samples. The scattered intensities were measured as a function of θ, the scattering

angle. The sample-detector distance was set to 1.7 m. Calibration of the detector was carried out with rat tail and cholesterol. From the scattering angle the scattering vector (Q) was calculated $Q = 4\pi(\sin\theta)/\lambda$, in which λ is the wavelength of 0.154 nm at the sample position. The diffraction curves were plotted as a function of Q. In this way a lamellar phase can be characterized by a number of peaks at the same interpeak distance. Every peak is characterized by its spacing calculated from its position as follows: spacing = $2\pi/Q_n$. From the positions of a series of peaks (Q_n) the periodicity of a lamellar phase was calculated using the equation $Q_n = 2\pi n/d$, in which d is the periodicity and n the order of the diffraction peak. The diffraction patterns were normalized with respect to the synchrotron beam intensity decay. The static measurements were carried out during a period of 15 min. When the temperature-induced lipid phase changes were examined, the temperature was raised from 25° to 95°C with a heating rate of 2°C/min. The data for each diffractogram were collected for 1 min.

Wide angle X-ray diffraction. The diffraction patterns were obtained with the fibre diffraction camera at station 7.2 of the synchrotron radiation source in Daresbury. A more detailed description of this station is given in elsewhere (11). The X-ray path-length through the sample was 1 mm. The read-out thermocouple was inserted in the sample cell. The sample to film distance was set to 0.11 m. The wavelength of the X-rays at the position of the sample was 0.1488 nm. The positions of the reflections are denoted by its spacings in real space.

RESULTS

Long range ordering at room temperature

Ceramides were separated from other pig SC lipids by column chromatography. The ceramide profile is given in **Table 1.** The chain length distribution of the (α-hydroxy) fatty acids amide-linked to the ceramides is given in **Table 2.** For the experiments, cholesterol and isolated pig SC ceramides were mixed in molar ratios varying between 0 and 2.0. The absence of cholesterol anhydride reflections in the wide-angle diffraction pattern indicated that the lipids were hydrated throughout the whole sample.

The SAXD measurements (**Fig. 1**) revealed that in the absence of cholesterol, isolated ceramides did not show a long range ordering; only a small shoulder at a descending scattering curve was observed. Upon addition of cholesterol to reach a cholesterol/ceramide (CHOL/CER) molar ratio of 0.1, a 5.9 nm diffraction peak ($Q = 1.07\ nm^{-1}$) was detected with a small shoulder on the right hand side with a spacing of 4.3 nm. Increase in the cholesterol content to a CHOL/CER ratio of 0.2 resulted in the appearance of three strong reflections corresponding to a spacing of 12.3 nm ($Q = 0.51\ nm^{-1}$), 5.56 nm ($Q = 1.13\ nm^{-1}$), 4.26 nm ($Q = 1.47\ nm^{-1}$), respectively, and one weak 1.76 nm reflection at $Q = 3.56\ nm^{-1}$. The 5.56 nm peak was not symmetric, but exhibited a small shoulder on the left-hand side. The 12.3, 4.26, and 1.76 nm reflections are most probably the first, third, and seventh order diffraction peaks of a lamellar phase with a periodicity of approximately 12.2 nm. At the CHOL/CER molar ratio of 0.2, an additional weak reflection was occasionally found at 3.38 nm ($Q = 1.86\ nm^{-1}$) indicating the presence of crystalline cholesterol. At CHOL/CER molar ratio of 0.4, two peaks at spacings of 6.2 and 5.3 nm instead of the asymmetric 5.56 nm peak were detected. Higher order reflections of both phases were detected on the diffraction curves (**Table 3**) at 2.65 nm (second order 5.3 nm phase) and 2.09 nm (6th order of the 12.2 nm lamellar phase). The presence of the 2.65 nm reflection indicated that the 5.3 nm phase was also lamellar. Further increase in choles-

TABLE 3. Phases and corresponding spacings in cholesterol/ceramide mixtures, as measured by SAXD and WAXD at room temperature

Composition	Spacings in nm		
CHOL:CER molar ratio	12.2 nm Phase	5.2 nm Phase	Chol
0:1.0	–	–	–
0.1:1.0	5.9, 4.3	–	–
0.2:1.0	12.3(1), 5.56(2), 4.3(3),	5.56(1)	3.38
0.4:1.0	12.4(1), 6.2(2), 4.2(3), 2.09(6), 1.77(7)	5.30(1), 2.65(2)	3.33
0.6:1.0	12.0(1), 6.08(2), 4.15(3), 2.09(6), 1.77(7), *1.53(8)*	5.21(1), 2.61(2)	3.36, 1.68
1.0:1.0	12.0(1), 5.98(2), 4.17(3), 2.10(6), 1.78(7), *1.58(8), 1.47(9), 1.12(11)*	5.28(1), 2.64(2)	3.35, 1.67
2.0:1.0	13.2(1), 6.2(2), 4.2(3)	5.32(1	3.32, 1.67

Numbers in italics show phases/spacing only observed in the WAXD pattern; Chol, cholesterol reflections.

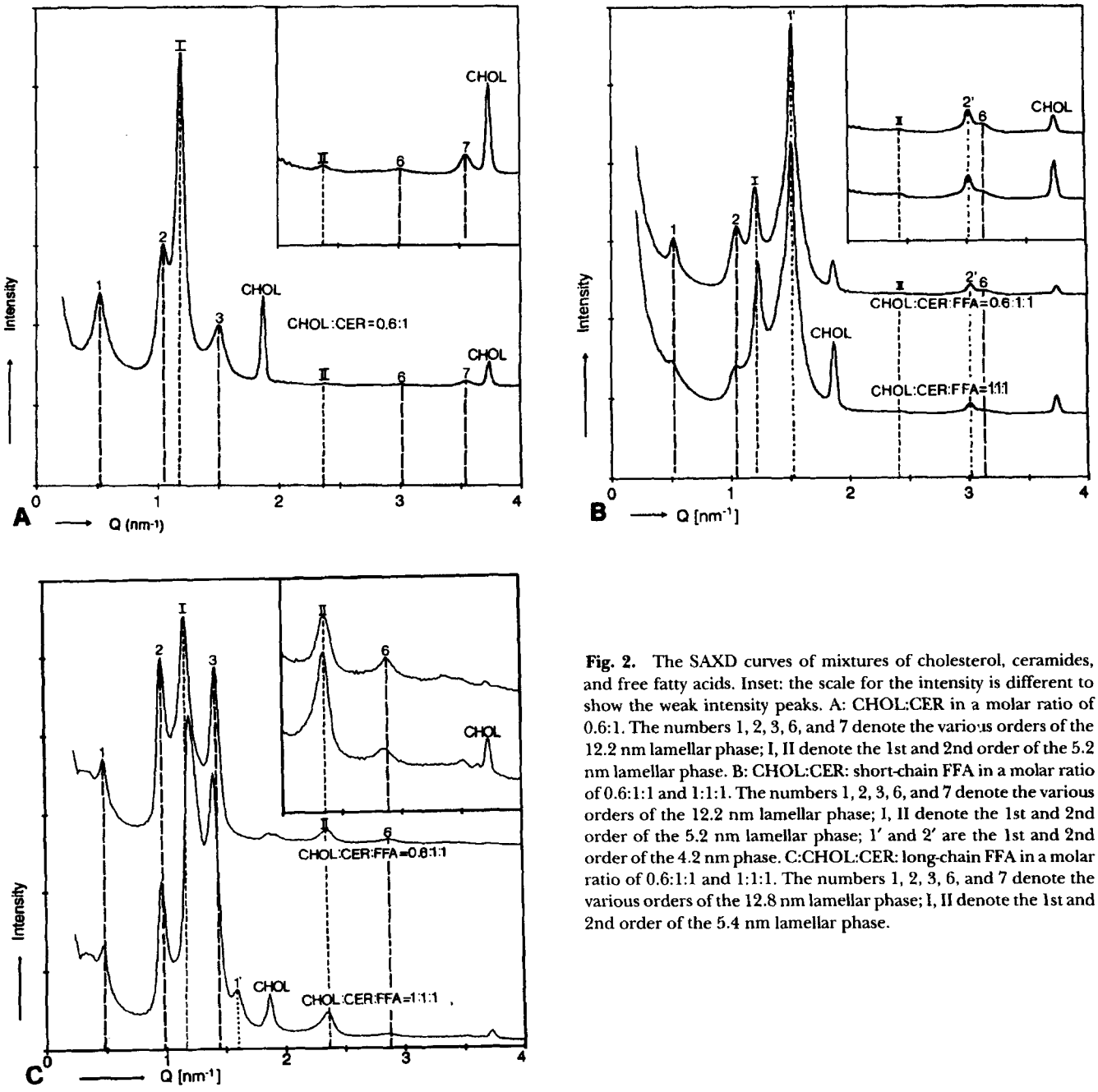

Fig. 2. The SAXD curves of mixtures of cholesterol, ceramides, and free fatty acids. Inset: the scale for the intensity is different to show the weak intensity peaks. A: CHOL:CER in a molar ratio of 0.6:1. The numbers 1, 2, 3, 6, and 7 denote the various orders of the 12.2 nm lamellar phase; I, II denote the 1st and 2nd order of the 5.2 nm lamellar phase. B: CHOL:CER: short-chain FFA in a molar ratio of 0.6:1:1 and 1:1:1. The numbers 1, 2, 3, 6, and 7 denote the various orders of the 12.2 nm lamellar phase; I, II denote the 1st and 2nd order of the 5.2 nm lamellar phase; 1′ and 2′ are the 1st and 2nd order of the 4.2 nm phase. C:CHOL:CER: long-chain FFA in a molar ratio of 0.6:1:1 and 1:1:1. The numbers 1, 2, 3, 6, and 7 denote the various orders of the 12.8 nm lamellar phase; I, II denote the 1st and 2nd order of the 5.4 nm lamellar phase.

terol content to a CHOL/CER molar ratio of 0.6 did not result in significant changes in the positions of the various diffraction peaks, but the intensity of the cholesterol peak increased. Furthermore, one additional weak 1.53 nm reflection appeared (observed in the WAXD pattern), which can be interpreted as the 8th order reflection of the 12.2 nm phase. An increase in cholesterol content to a CHOL/CER molar ratio of 1.0 did not induce changes in the diffraction profile in the small-angle region. However, at this molar ratio even the 9th and 11th order peaks (observed in the WAXD pattern) of the 12.2 nm phase were detected, indicating that at this CHOL/CER ratio the 12.2 nm lamellar phase is very well ordered. At a CHOL/CER molar ratio of 2.0, the intensities of peaks based on the 12.2 nm phase decreased drastically as compared to those seen at a CHOL/CER ratio of 1.0 (not shown), strongly suggesting that at a high cholesterol content the 12.2 nm lamellar phase disappeared, while the 5.2 nm phase remained.

Next to cholesterol and ceramides, FFA are the main constituents of the SC lipids (19, 20). Therefore, additional measurements were carried out with CHOL/CER/FFA mixtures. Two different FFA mixtures were used. The composition of short-chain FFA and long-chain FFA mixtures were based on the earlier published data by Lampe, Williams, and Elias (22) and Wertz and Downing (12), respectively.

As shown in **Fig. 2** and **Table 4,** when short-chain FFA were added to reach a CHOL/CER/FFA molar ratio of 0.6:1.0:1.0, the 4.23 nm peak (Q = 2.33 nm^{-1}) increased in intensity and an additional peak was found at a spacing of 2.11 nm. The changes in the diffraction curve can be ascribed to a formation of a new phase in the mixture considering the following observations. *i)* The 4.2 nm peak intensity increased significantly, whereas the intensity of other peaks, originally based on the same phase, did not change. *ii)* From the shape of the 4.2 nm peak it can be deduced that the peak is composed from two peaks, of which the strongest peak showed the smallest peak width at the half maximum intensity. *iii)* A second order reflection was found at 2.11 nm that was not present at the diffraction curve of the CHOL/CER mixture at a molar ratio of 0.6 (see Fig. 2). *iv)* In addition, the WAXD pattern revealed the presence of higher order reflections at 1.39 (3rd order) and 1.04 (4th order) nm (see below). The positions of other peaks were similar to those seen with the CHOL/CER mixture at a molar ratio of 0.6. Increasing the cholesterol content to achieve an equimolar CHOL/CER/FFA mixture, resulted in a strong reduction in the intensity of the reflections based on the 12.2 nm phase while the intensity of reflections based on the 5.2 nm phase remained unchanged. In addition the WAXD pattern revealed a 5th order reflection of the 4.23 nm phase at 0.83 nm.

In contrast to mixtures with short-chain FFAs, when a mixture of long-chain FFA was added to reach a CHOL/CER/FFA molar ratio of 0.6:1:1 no additional phase was formed (see Fig. 2c). However, a slight shift of several positions of peaks to smaller Q-values was observed as compared to peak positions seen with the CHOL/CER mixture at a molar ratio of 0.6. The high intensity peaks based on the long periodicity phase were located at 13 nm (Q = 0.48 nm^{-1}), 6.41 nm (Q = 0.98 nm^{-1}), and 4.39 nm (Q = 1.43 nm^{-1}), respectively, revealing a periodicity of 12.9 nm, while the high intensity peaks based on the short periodicity phase were located at 5.30 nm (Q = 1.19 nm^{-1}) and 2.66 nm (2.35 nm^{-1}) revealing a repeat distance of 5.3 nm. Increase in the CHOL content to an equimolar CHOL/CER/FFA mixture resulted in a further small shifts in the peak positions of both phases. The 1st, 2nd, and 3rd order diffraction peaks based on the long periodicity phase were now located at 13.2 nm (Q = 0.476 nm^{-1}), 6.49 nm (Q = 0.96 nm^{-1}), and 4.44 nm (Q = 1.39 nm^{-1}), respectively, indicating a periodicity of 13.1 nm. The 1st and 2nd order peaks of the short periodicity phase were located at a spacing of 5.19 nm (Q = 1.20 nm^{-1}) and 2.66 nm (Q = 2.38 nm^{-1}), respectively, revealing a 5.3 nm lamellar phase. In addition, a small peak was present at a spacing of 3.96 nm (Q = 1.58 nm^{-1}). This peak cannot be ascribed to FFA, as pure FFA reveal a phase with a

TABLE 4. Phases and corresponding spacings in cholesterol/ceramide/free fatty acid mixtures as measured by SAXD and WAXD at room temperature

CHOL:CER:FFA Molar Ratio	Spacings (nm)/(order)			
Short-Chain FFA	12.2 nm Phase	5.1 nm Phase	4.2 nm Phase	Chol
0.6:1:1	12.5(1), 5.96(2), 4.12(3), 2.08(6)	5.08(1), 2.60(2	4.23(1), 2.11(2) 1.37(3), 1.04(4)	3.36, 1.68
1:1:1	12.0(1), 5.98(2), 4.17(3), 2.09(6) 1.77(7)	5.17(1), 2.59(2	4.23(1), 2.13(2) 1.39(3), 1.05(4) 0.83(5)	3.36, 1.68
Long-chain FFA	13.0 nm Phase	5.3 nm Phase		Chol
0.6:1:1	13.0(1), 6.41(2), 4.39(3), 3.23(4) 2.18(6), 1.88(7)	5.30(1), 2.66(2), 1.78(3)		3.36, 1.68
1:1:1	13.3(1), 6.49(2), 4.44(3), 2.19(6	5.20(1), 2.67(2), 1.79(3)		3.36, 1.68

Chol, cholesterol reflections.

periodicity of 3.7 nm. A very likely explanation is that at a high CHOL and FFA content a new phase from CHOL and FFA is formed.

Lateral hydrocarbon packing of the ceramide mixtures

In the absence of cholesterol, ceramides showed a crystalline packing that can be deduced from the diffraction pattern as reflections could be observed at 0.446, 0.435, 0.39, 0.358, 0.345, 0.332, and 0.311 nm. Addition of cholesterol changed the diffraction pattern dramatically. In the diffraction pattern of a CHOL/CER mixture with a molar ratio of 0.1, a broad reflection at 0.41 nm could be detected, indicating a hexagonal lateral packing (**Fig. 3**). Increasing the cholesterol content to CHOL/CER molar ratio of 0.2 resulted in a diffraction profile consisting of various weak but sharp diffraction rings. The strongest reflections were found at 0.599, 0.586, and 0.380 nm spacings, corresponding to the strongest reflections of cholesterol monohydrate. The 0.41 nm reflection was still present. A further increase in the relative amount of cholesterol resulted in an increased intensity of the cholesterol reflections (**Fig. 4**). The finding that upon increasing the cholesterol content the 0.41 nm reflection did not change in position suggests that an increase in cholesterol content does not result in a transition of lipids from hexagonal to a liquid ordered phase. However, it seems that the 0.41 nm

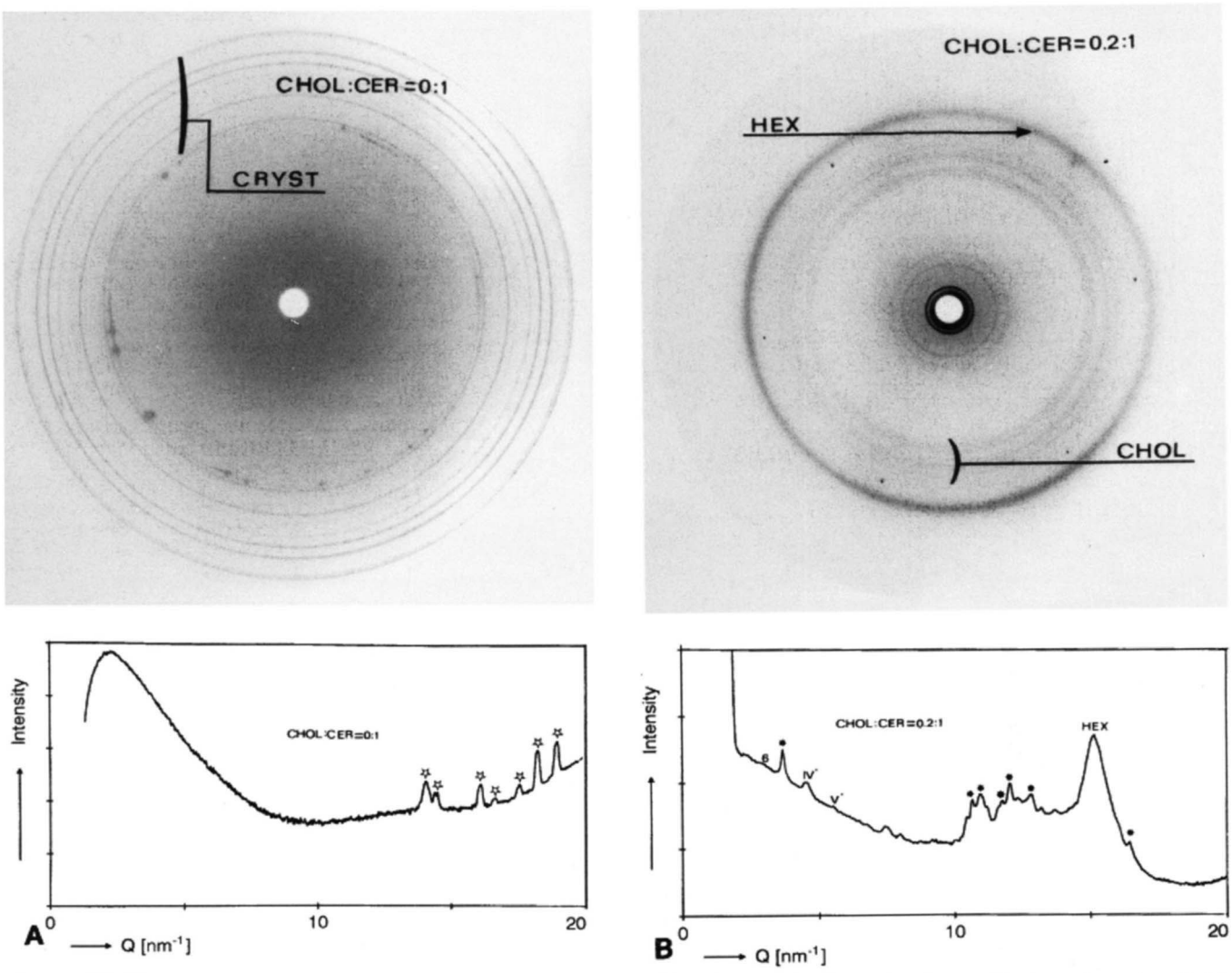

Fig. 3. WAXD pattern and the densitometer scan of (A) ceramides and (B) a mixture of cholesterol and ceramides in molar ratio of 0.2:1. CRYST, reflections of the crystalline phase; HEX, 0.410 nm reflection based on a hexagonal lateral packing. In the densitometer scan the IV′ and V′ denote the 4th and 5th orders of the 5.6 nm phase and 6 the 6th order of the 12.2 nm phase. CHOL, cholesterol.monohydrate reflections. In the densitometer scan the cholesterol reflections are indicated by a *, and the crystalline reflections by a (star).

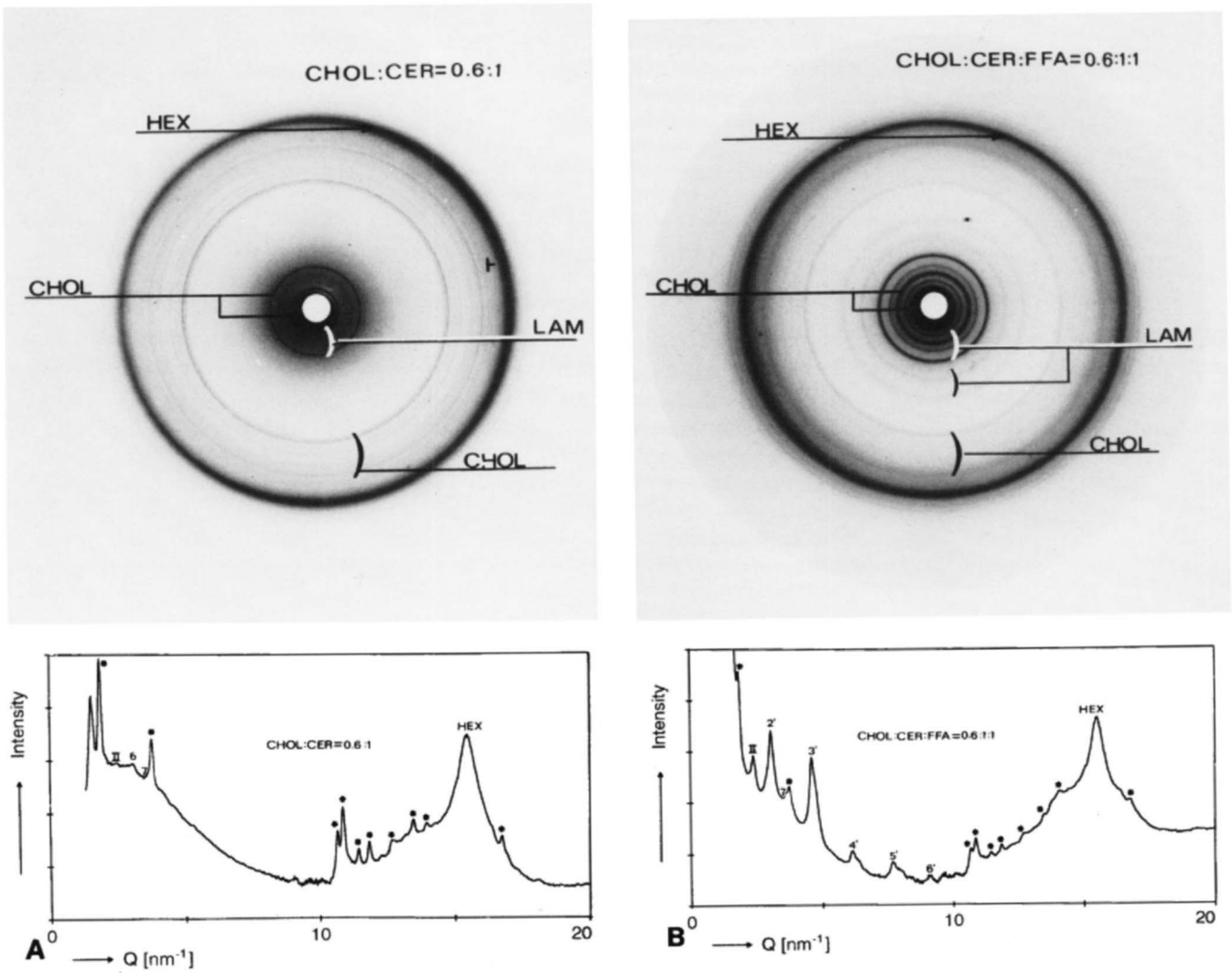

Fig. 4. The WAXD pattern and the densitometer scan of mixtures of (A) CHOL:CER mixed in a molar ratio of 0.6:1 and (B) CHOL:CER:short-chain FFA mixed in a molar ratio of 0.6:1:1. HEX, the 0.410 nm reflection based on a hexagonal lateral packing; LAM, reflections based on the lamellar phases. In the densitometer scan 6 and 7 refers to the higher order reflections of the 12.2 nm lamellar phase, II denotes the 2nd order of the 5.2 nm lamellar phase, and 2′, 3′, 4′, 5′, and 6′ refer to the orders of the 4.2 nm phase. CHOL, reflections based on cholesterol monohydrate. In the densitometer these reflections are indicated by *.

reflection broadens upon increasing the cholesterol content, indicating a slight disordering of the lateral packing.

When short-chain FFA were added to CHOL/CER mixtures, no changes in the lateral packing was observed, except for a small decrease in the width of the 0.41 nm reflection. The reflections corresponding to cholesterol decreased in intensity, suggesting improved solubilization of the cholesterol in the presence of FFA. This finding is in accordance with data obtained with SAXD.

Temperature-induced changes in long-range order

The diffraction data of equimolar CHOL/CER mixtures were collected during heating the lipid sample from 25° to 95°C at a heating rate of 2°C/min. Each minute an X-ray diffractogram was recorded. This approach enabled us to follow the phase changes as a function of temperature in detail. In the SAXD pattern, weak reflections could not be detected due to the short exposure time used for monitoring of the diffractograms and at 25°C only 4.17 nm, 5.28 nm, 5.96 nm, and 12.0 nm diffraction peaks were observed (**Fig. 5**). Increasing the temperature caused the disappearance of the 12.0 and 5.96 nm reflections in the temperature range between 65° and 70°C, indicating that these two reflections originate from the same 12.2 nm lamellar phase. In this temperature range also, a slight increase in spacing from 12.0 to 13.0 nm was observed. The 5.28 nm diffraction peak disappeared between 55° and 60°C, indicating that this peak originates from another phase than the 12.0 and 5.96 nm peaks. In the temperature range between 50° to 55°C, the position of 4.17 nm peak shifted to lower Q values corresponding to a spacing of 4.4–4.6 nm. In this temperature range the peak intensity markedly increased. Further increase in temperature

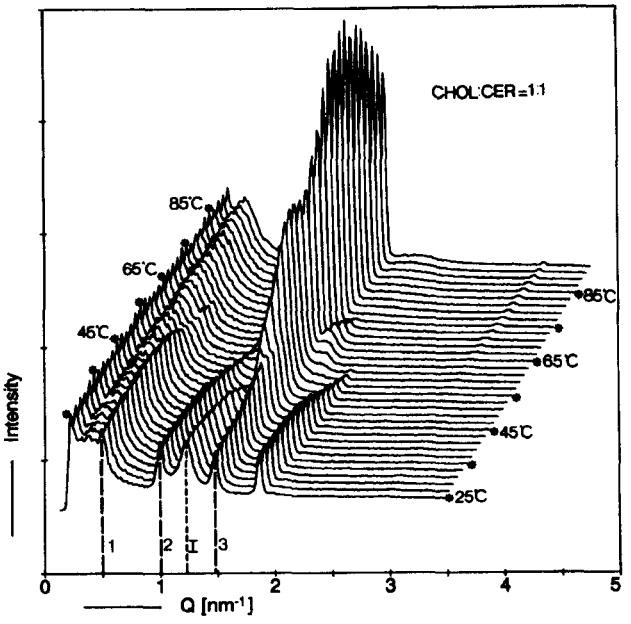

Fig. 5. The temperature-induced changes in SAXD profiles. The heating rate is 2°C/min. A mixture of CHOL:CER in a molar ratio of 1:1. Temperatures are indicated in the figure. In each sequential curve the temperature was raised by 2°C. 1, 2, and 3 refer to the 1st, 2nd, and 3rd order of the 12.2 nm phase; I refers to the 1st order of the 5.2 nm phase. The amount of material available for the measurements was limited which resulted in a decrease in signal-noise ratio in the X-ray curve.

was accompanied by disappearance of this diffraction peak between 80° and 85°C.

DISCUSSION

Recent studies on the phase behavior of lipids in intact pig SC (10) revealed that in pig SC at least two lamellar phases were present with periodicities of 6.0 and 13.2 nm, respectively. Upon increasing the water content in the SC from 20 to 60% w/w, the bilayers did not swell (8) but a phase separation occurred between lipids and water (23). These results clearly indicate that the amount of water located between the lipid bilayers in the SC is limited. We can therefore expect that although the lipid mixtures were prepared in an excess of buffer solution, the amount of water present between the lipid lamellae was low.

When cholesterol was added to ceramides isolated from pig SC, two lamellar phases with a periodicity of approximately 5.2 and 12.2 nm have been detected at CHOL/CER molar ratio larger than 0.4. Similar lamellar ordering has been observed in intact SC. Our results further indicate that even very low amounts of cholesterol seem to be sufficient for lamellar lipid organization as already at CHOL/CER molar ratio of 0.1, a 5.9 nm diffraction peak with a small shoulder on the right-hand side with a spacing of 4.3 nm could be detected. The presence of this shoulder indicates that the 12 nm phase, present in mixtures with a higher CHOL/CER molar ratio, also exists in this mixture. As the width at half maximum intensity of the 5.9 nm peak was quite large, we speculated that the reflection corresponding to a 5.9 nm spacing might have been composed of two reflections. Slight increase in cholesterol content to a CHOL/CER molar ratio of 0.2 resulted, indeed, in the appearance of a strong reflection at 5.6 nm consisting of a major peak with a small shoulder on the left-hand side and the reflections of the 12.2 nm phase were more clearly present. At the CHOL/CER molar ratio of 0.4, two peaks at 6.2 nm and 5.3 nm spacing were observed. The change from an asymmetric 5.6 nm peak to a doublet with spacings of 6.2 and 5.3 nm strongly suggests that this change is mainly due to a shift in peak position from 5.6 to 5.3 nm spacing and that therefore the formation of the 5.2 nm lamellar phase requires higher cholesterol contents than the formation of the 12.2 nm lamellar phase. At a CHOL/CER molar ratio of 2.0, the diffraction peaks based on the 12.2 nm phase decreased in intensity as compared to the 5.2 nm diffraction peak. These findings suggest that the 5.2 nm lamellar phase dominates at very high cholesterol contents.

Comparing the diffraction pattern of the intact SC with that of the CHOL/CER mixtures (**Fig. 6**), led us to conclude that the first order diffraction peak found in the diffraction patterns of CHOL/CER mixtures is also present as a weak shoulder at the descending scattering curve of intact SC. Furthermore, the higher order diffraction peaks of the 12.2 nm and 13.2 nm phases of CHOL/CER mixtures and SC, respectively, are also present in the diffraction patterns. However, whether or not the diffraction peaks at 4.2, 5.2, and 6.0 nm detected with CHOL/CER mixtures are also present in the intact SC needs some elucidation. The peak width at half maximum intensity is proportional to $(Nd)^{-1}$, in which N is the number of repeating units and d is the periodicity of the phase. The finding that the number of lamellae in the intercorneocyte space is very limited (24) explains why the peak width at half maximum intensity in intact SC is large and why the resolution in the diffraction pattern of intact SC is very poor. Contrary to SC, in isolated lipid mixtures the number of repeating units in various stacks is not limited by the available space between the cells. This means that the peak width at half maximum intensity is much smaller in the diffraction curve of the isolated lipid mixtures and that the resolution of the various peaks in the diffraction pattern increases. This may explain why two partly resolved peaks with spacings of approximately 5.2 and 6.0 nm observed in the diffraction profile of the isolated

lipid mixtures turn into one broad peak in SC where N is low. Indeed, a broad peak corresponding to a spacing of 6 nm was observed in the diffraction curve of intact pig SC. In addition, the fully separated 4.3 nm peak in the diffraction curves of the CHOL/CER mixtures most likely corresponds to the shoulder observed in the diffraction curve of intact SC at approximately 4.4–4.5 nm spacing. Furthermore, in pig SC a hexagonal lateral packing of the lipids was also found. From these observations we conclude that at room temperature the phase behavior of cholesterol mixed with isolated ceramides in molar CHOL/CER ratios ranging between 0.4 and 1.0 was close to that found in intact SC.

To further demonstrate the similarity in lipid phase behavior of the CHOL/CER mixtures and of the SC, we compared the intensities of various peaks of the 12.2 nm and 13.2 nm lamellar phases. The results given in **Table 5,** show that the relative intensities of peaks based on the long periodicity phases in intact SC and CHOL/CER lipid mixtures show the same trend. This indicates that the localization of lipids in the CHOL/CER mixtures within the 12.2 nm phase is very similar to that within the 13.2 nm phase in intact SC and most probably corresponds to two broad and one narrow low-electron-density regions observed in transmission electron microscopy (10). The small difference in periodicities between the CHOL/CER mixtures and the SC is most probably due to the presence of long-chain free fatty acids in the latter (see below).

It should be noted that only two diffraction peaks based on the short periodicity phase could be detected in the diffraction patterns of both the CHOL/CER mixtures and the intact SC, a first order high intensity peak and a second order low intensity diffraction peak. This strongly indicates that this short periodicity phase is less ordered than the long periodicity phase in both the CHOL/CER mixtures and the SC, again reflecting the similarity in lipid phase behavior in both samples. The similarity was even more pronounced when long-chain FFAs were added to CHOL/CER mixtures. Namely, the long-chain FFAs most probably intercalate within both lamellar phases which results in a slight increase in the periodicities from 5.2 and 12.2 nm to approximately 5.3 and 13.0 nm, respectively. In contrast, when short-chain FFA were added, the phase behavior of CHOL/CER/FFA resembled the phase behavior of lipids in intact SC to a lesser extent than the CHOL/CER mixtures. A prominent peak was observed in the CHOL/CER/FFA mixtures at a 4.2 nm spacing that has never been seen in intact SC. The observed changes in the diffraction pattern can be ascribed to a formation of a new phase in the mixture. Most likely this is due to a mismatch in fatty acid chain length of FFA and of CER (see Table 2), as in these experiments a mixture of short-chain FFA (with palmitic acid as a major component) was used. Such mixtures have been often used in studies with skin–lipid model systems (25–30). In addition, in the presence of short-chain FFA the intensity of reflections based on 12 nm decreased markedly in equimolar CHOL/CER/FFA mixtures, while in the absence of FFA a similar decrease was observed in CHOL/CER mixtures at a much higher cholesterol content, namely at a molar ratio of 2.0.

The results of the present study clearly indicate that the phase behavior remains essentially unchanged over a wide range of CHOL/CER/long-chain FFA molar ratios, suggesting that for proper organization of SC lipids the presence of equimolar amounts of cholesterol, ceramides, and free fatty acids is not required. This finding also explains why small variations in the CHOL/CER molar ratios, as measured in lipids extracted from SC originating from different donors, only marginally affected the lipid phase behavior. Furthermore, it indicated that the presence of hydrocarbons, sterol esters and di- and triglycerides is not required for the formation of lamellar structures within the intercorneocyte space. This observation is in agreement with earlier studies that showed that upon removal of large amounts of nonpolar lipids the SC barrier function was only marginally perturbed, while after the removal of ceramides and cholesterol the barrier function was markedly changed (31).

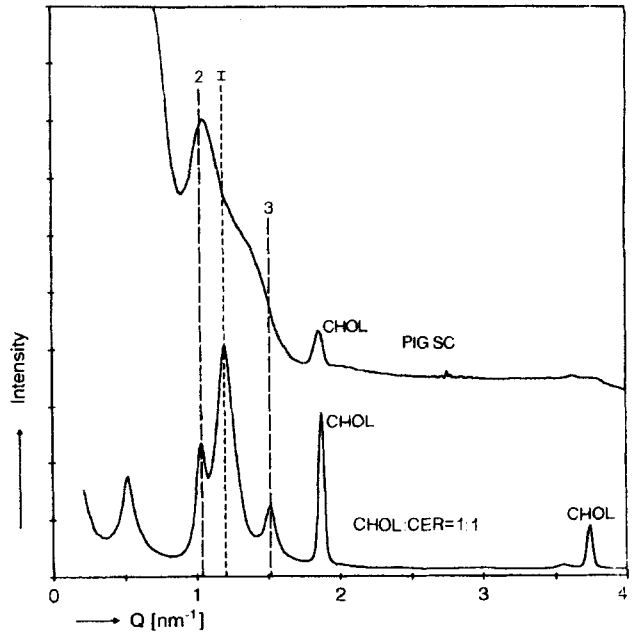

Fig. 6. The SAXD profile of intact pig stratum corneum (SC) and of a mixture of cholesterol and ceramides in a 1:1 molar ratio. The high intensity at low Q value ($Q < 0.5$ nm^{-1}) observed in the diffraction curve of intact SC is due to the presence of keratin inside the corneocytes. 2 and 3 refer to the 2nd and 3rd order of the 12.2 nm lamellar phase; I denotes the 1st order of the 5.2 nm phase; CHOL refers to cholesterol.

TABLE 5. Relative intensities of the diffraction peaks of the 12.2 nm phase of equimolar CHOL/CER mixtures and of the 13.2 nm phase of the stratum corneum

Order of Diffraction Peak	CHOL/CER Mixture 12.2 nm Lamaellar Phase	Stratum Corneium 13.2 nm Lamellar Phase
1	1.0	1.0
2	1.3	1.12
3	0.7	1.0
4	0.015	0.045
5	0.007	0.02
6	0.016	0.017
7	0.015	0.003

For scaling, the intensity of the first order diffraction peak of both phases was set equal to 1.0.

Our results strongly indicate that both the short-chain and long-chain FFAs affect the lipid behavior by increasing the solubility of cholesterol in the lamellar structures, as the intensity of cholesterol reflections corresponding to crystalline cholesterol is decreased in CHOL/CER/FFA mixtures. The presence of cholesterol in solubilized form is most probably a prerequisite for proper functioning of the SC barrier. Namely, when SC contains relatively low amounts of FFA, as it is the case for lamellar ichthyosis patients, a substantial amount of cholesterol is present in a crystalline form, as can be deduced from the presence of the diffraction peak at a 3.35 nm spacing, and the SC function is perturbed (32). Furthermore, a change in the periodicity of lipid phases observed earlier in the diseased skin (32) cannot be ascribed to a changed CHOL/CER molar ratio but to *i)* changes in the relative amounts of various ceramide classes or *ii)* a higher abundance of fatty acids with a shorter chain length (present either as free fatty acids or bound to ceramides).

In earlier studies (7–9) it was suggested that proteins might be very important for proper lipid organization in the SC. These suggestions were based on two observations: *i)* lipid phase behavior found in SC could not be mimicked with SC lipids extracted from mouse or pig SC, and *ii)* electron density calculations revealed the existence of very large high-electron-density regions that could not be explained by the presence of SC lipids that only possess small head groups. However, this study shows for the first time that two lamellar phases can be formed in the absence of proteins with a mixture of isolated ceramides and cholesterol, indicating that the presence of proteins is not required for the formation of these lipid lamellar phases.

More detailed information on the lipid phase behavior can be obtained when the phase behavior is examined as a function of temperature. These experiments revealed that the diffraction peaks of the 12.2 nm phase disappeared between 65° and 70°C. The first order diffraction peak of the lamellar phase with a periodicity of 5.2 nm disappeared between 55° and 60°C (10). In intact SC these phases disappeared in the same temperature range. In contrast, in the equimolar CHOL/CER mixture, the 4.3 nm peak increased substantially in intensity between 50° and 70°C and the peak position shifted to longer spacings, suggesting that at approximately 50°C a new phase has been formed. The periodicity of this new phase is approximately 4.2 nm. In intact pig SC, we also observed a slight increase of the 4.5 nm peak at 50°C, which might suggest a similar phase behavior as seen with isolated lipids. However, in intact SC this peak already disappeared at 55°C indicating that the situation is different than with isolated lipids.

In recent studies (27, 29) crystalline phases were found in an equimolar mixture of brain ceramide-3/CHOL/palmitic acid. The formation of these crystalline phases and the hexagonal lateral phase observed in those studies might be due to the formation of intermolecular hydrogen bonds in ceramide/cholesterol mixtures, because in another study (33), in which the interaction between pure ceramides arranged in monolayers was examined, it was found that condensation of hydrocarbon chains of the ceramides occurred due to the formation of intermolecular hydrogen bonds. It should be noted that the presence of crystalline phases is of great importance for the water-holding capacity of the SC (34) and for the barrier function of the SC, as the diffusional resistance of crystalline phases is much larger than that of liquid phases. The presence of crystalline phases is very exceptional in biological membranes. In most cell membranes a liquid lateral packing has been found. This liquid phase was frequently demonstrated in cholesterol/phospholipid mixtures that served as a model for membranes. For example, in mixtures of cholesterol and phospholipids or cholesterol and sphingomyelin the crystalline or hexagonal phases have not been observed. In most cases only an ordered liquid phase was detected when the cholesterol/phospholipid or cholesterol/sphingomyelin molar ratio exceeded 0.33 (35, 36).

Parrott and Turner (14) reported the presence of two lamellar phases similar to those present in SC in dry mixtures of cholesterol and brain ceramide-3. When we prepared hydrated mixtures of cholesterol and brain ceramide-3 using an acetate buffer at pH 5 (the pH value also found in the SC) we observed only one phase with a periodicity of 4.7 nm (unpublished results). Our findings are in accordance with those of Schückler et al. (26) and Lieckfeldt et al. (37) who also found only one lamellar phase with a periodicity ranging between 5 and 6 nm in hydrated equimolar mixtures of cholesterol, brain ceramide-3 and free fatty acids.

In summary, the results of the present study clearly show that mixtures of CER/CHOL and CER/CHOL/long-chain FFA closely mimic the lipid phase behavior in intact SC. The phase lipid behavior studies with lipid mixtures in which relative amounts of individual components are changed over a wide range (a condition that cannot be achieved in vivo) enable us to broaden our knowledge on the role various skin lipids play in the organization of the lipid phases. This may contribute to better understanding of mechanisms governing the SC lipid organization and phase behavior in both healthy skin and diseased skin.

Manuscript received 5 October 1995, in revised form 27 November 1995, and in re-revised form 5 February 1996.

REFERENCES

1. Elias, P. M. 1983. Epidermal lipids, barrier function, and desquamation. *J. Invest. Dermatol.* **80:** 44s–49s.
2. Menon, G. P., K. R. Feingold, and P. M. Elias. 1992. Lamellar body secretory response to barrier disruption. *J. Invest. Dermatol.* **98:** 279–289.
3. Swanbeck, G. 1959. Macromolecular organisation of epidermal keratin. *Acta Dermato-Venereol. Suppl.* **39:** 5–37.
4. Swanbeck, G. 1961. X-ray diffraction of scales from different dermatoses. *Acta Dermato-Venereol.* **41:** 289–296.
5. Breathnach, A. S., T. Goodman, C. Stolinky, and M. Gross. 1973. Freeze fracture replication of cells of stratum corneum of human epidermis. *J. Anat.* **114:** 65–81.
6. Swartzendruber, D. C., P. W. Wertz, D. J. Kitko, K. C. Madison, and D. T. Downing. 1989. Molecular models of intercellular lipid lamellae in mammalian stratum corneum. *J. Invest. Dermatol.* **92:** 251–257.
7. White, S. H., D. Mirejovsky, and G. I. King. 1988. Structure of lamellar lipid domains and corneocytes envelopes of murine stratum corneum. An X-ray diffraction study. *Biochemistry.* **27:** 3725–3732.
8. Bouwstra, J. A., G. S. Gooris, J. A. van der Spek, and W. Bras. 1991. The structure of human stratum corneum as determined by small angle X-ray scattering. *J. Invest. Dermatol.* **96:** 1006–1014.
9. Bouwstra, J. A., G. S. Gooris, J. A. van der Spek, S. Lavrijsen, and W. Bras. 1994. The lipid and protein structure of mouse stratum corneum: a wide and small angle diffraction study. *Biochim. Biophys. Acta.* **1212:** 183–192.
10. Bouwstra, J. A., G. S. Gooris, W. Bras, and D. T. Downing. 1995. Lipid organization in pig stratum corneum. *J. Lipid Res.* **36:** 685–695.
11. Bouwstra, J. A., G. S. Gooris, M. A. Salomons-de Vries, J. A. van der Spek, and W. Bras. 1992. Structure of human stratum corneum: a wide-angle X-ray diffraction study. *Int. J. Pharm.* **84:** 205–216.
12. Wertz, P. W., and D. T. Downing. 1991. Epidermal lipids. *In* Physiology, Biochemistry and Molecular Biology in the Skin. 2nd Edition. L. A. Goldsmith, editor. Oxford University Press, Oxford. 205–236.
13. Schürer, N. Y., and P. M. Elias. 1991. The biochemistry and function of stratum corneum lipids. *Adv. Lipid Res.* **24:** 27–56.
14. Parrott, D. T., and J. E. Turner. 1993. Mesophase formation by ceramides and cholesterol. *Biochim. Biophys. Acta.* **1147:** 273–276.
15. Holleran, W. M., M. Q. Man, W. N. Gao, G. P. Menon, P. M. Elias, and K. R. Feingold. 1991. Sphingolipids are required for mammalian epidermal barrier function. *J. Clin. Invest.* **88:** 1338–1345.
16. Man, M. Q., P. M. Elias, and K. R. Feingold. 1993. Fatty acids are required for epidermal permeability barrier function. *J. Clin. Invest.* **92:** 791–798.
17. Holleran, W. M., M. Q. Man, W. N. Gao, G. P. Menon, P. M. Elias, and K. R. Feingold. 1991. Sphingolipids are required for mammalian epidermal barrier function. *J. Clin. Invest.* **88:** 1338–1345.
18. Bligh, E. G., and W. J. Dyer. 1959. A rapid method of total lipid extraction and purification. *Can. J. Biochem. Physiol.* **37:** 911–917.
19. Ponec, M., A. Weerheim, J. Kempenaar, A. M. Mommaas, and D. H. Nugteren. 1988. Lipid composition of cultured human keratinocytes in relation to their differentiation. *J. Lipid Res.* **29:** 949–962.
20. Wertz, P. W., and D. T. Downing. 1983. Acylglucosylceramides of pig epidermis: structure determination. *J. Lipid Res.* **24:** 753–758.
21. Aly, R., C. Shirley, B. Cumico, and H. I. Maibach. 1978. Effect of prolonged occlusion on the microbial flora, pH, carbon dioxide and transepidermal water loss on human skin. *J. Invest. Dermatol.* **71:** 378–381.
22. Lampe, M. A., M. L. Williams, and P. M. Elias. 1983. Human epidermis lipids: characterization and modulations during differentiation. *J. Lipid Res.* **24:** 131–140.
23. van Hal, D. A., E. Jeremiasse, F. Spies, H. E. Junginger, and J. A. Bouwstra. 199x. The structure of hydrated human stratum corneum by freeze fracture elctron microscopy. *J. Invest. Dermatol.* In press.
24. Swartzendruber, D. C., A. Manganaro, K. C. Madison, M. Kremer, P. W. Wertz, and C. A. Squier. 1995. Organisation of the intercellular spaces of porcine epidermal and palatal stratum corneum: a quantitative study emplying ruthenium tetroxide. *Cell & Tissue Res.* **279:** 271–276.
25. Friberg, S. E., and D. W. Osborne. 1985. Small angle X-ray diffraction patterns of stratum corneum and model structures of its lipids. *J. Dispersion Sci. Technol.* **6:** 486–495.
26. Schückler, F., J. A. Bouwstra, G. S. Gooris, and G. Lee. 1993. An X-ray diffraction study of some model stratum corneum lipids containing azone and dodecyl-L-pyroglutamate. *J. Controlled Release.* **23:** 27–36.
27. Thewalt, J., N. Kitson, C. Aroujo, A. MacKay, and M. Bloom. 1992. Models of stratum corneum intercellular membranes: the sphingolipid headgroup is a determinant

of phase behaviour of mixed lipid dispersions. *Biochim. Biophys. Res. Commun.* **188:** 1247–1252.

28. Abraham, W., and D. T. Downing. 1991. Deuterium NMR investigations of polymorphism in stratum corneum lipids. *Biochim. Biophys. Acta.* **1068:** 189–194.
29. Kitson, N., J. Thewalt, M. Lafleur, and M. Bloom. 1994. A model membrane approach to epidermal permeability barrier. *Biochemistry.* **33:** 6707–6715.
30. Mizushima, H., J-I. Fukusawa, and T. Suzuki. 1995. Thermotropic behavior of stratum corneum lipids containing a pseudo-ceramide. *Lipids.* **30:** 327–332.
31. Grubauer, G., K. R. Feingold, R. M. Harris, and P. M. Elias. 1989. Lipid content and lipid type as determinants of the epidermal permeability barrier. *J. Lipid Res.* **30:** 89–96.
32. Lavrijsen, A. P. M., J. A. Bouwstra, G. S. Gooris, A. Weerheim, H. E. Boddé, and M. Ponec. 1995. Skin barrier function and stratum corneum lipid organisation in patients with lamellar ichthyosis. *J. Invest. Dermatol.* **105:** 619–624.
33. Löfgren, H., and I. Pascher. 1977. Molecular arrangements of spingolipids. The monolayer approach. *Chem. Phys. Lipids.* **20:** 273–284.
34. Rawlings, A. V., I. A. Scott, C. R. Harding, and P. A. Bowser. 1994. Stratum corneum moistening properties at the molecular level. *J. Invest. Dermatol.* **103:** 731–740.
35. Engelman, D. M., and J. E. Rothman. 1972. The planar organisation of lecithin-cholesterol bilayers. *J. Biol. Chem.* **247:** 3694–3697.
36. McIntosh, T. J., S. A. Simon, D. Needham, and C-H. Huang. 1992. Interbilayer interactions between sphingomyelin/cholesterol bilayers. *Biochemistry.* **31:** 2020–2024.
37. Lieckfeldt, R., J. Villalain, J. C. Gomez-Fernandez, and G. Lee. 1993. Diffusivity of structural polymorphism in some stratum corneum model systems. *Biochim. Biophys. Acta.* **1151:** 182–188.